Biomedical Signal Processing and Control 68 (2021) 102627

Contents lists available at ScienceDirect

Biomedical Signal Processing and Control

journal homepage: www.elsevier.com/locate/bspc

Patient's intention detection and control for sit-stand mechanism of an assistive device for paraplegics

Ahmad Abdullah [a], Zareena Kausar [a], Aamer Hameed [b], Shakil R. Shiekh [a], Haroon Khan [c,*]

[a] Department of Mechatronics and Biomedical Engineering, Air University, Islamabad, Pakistan
[b] Department of Pulmonology and Critical Care Medicine, Services Institute of Medical Sciences, Services Hospital, Lahore, Pakistan
[c] Department of Mechanical, Electronics and Chemical Engineering (MEK), Oslo Metropolitan University, Pilestredet 46, 0167 Oslo, Norway

ARTICLE INFO

Keywords:
EEG
PID
Non-linear control
Sliding mode control
Chattering removal
Rehabilitation
Sit–stand

ABSTRACT

Rehabilitation and assistive technologies are touching new bounds of excellence due to the advent of more user friendly human–machine interfaces (HMI) and ergonomic design principles. Among the most fundamental movements which are required in performing activities of daily living is the sit and stand motion, a device is proposed in this study which enables a patient to perform his activities of daily living (ADL) tasks by enabling them to sit, stand and move without the need of an assistant. The device, in this study, is proposed to be activated by an electroencephalogram (EEG) based intention acquisition system. The intention is acquired from eye blinks. The EEG based intention detection system converts eye blinks to respective commands after classification of eye blink signals collected using EMOTIVE® EPOCH^{+} headset. These control commands then trigger the control algorithm which then actuates and controls the system states. For the later, two control schemes namely proportional integral derivative (PID) control and sliding mode control (SMC) are tested in this study. The simulation and experimental results are given. The experimental setup consists of an offline EEG signal classification module, Simulink® model and the prototype of the actual device. It is concluded that SMC performs far better than PID for control of the assistive device in ensuring patient comfort during motion.

1. Introduction

Paraplegia is the paralysis of the lower extremity of the human body [1]. It is an impairment affecting either motor or sensory function of lower body. Rehabilitation is a process that aims to restore independence and self-determination in disabled individuals. Rehabilitation process involves various kinds of therapies and assistive mechanisms that are used for training of and exercises by disabled persons. The purpose of rehabilitation of the patients is to make them stand up and walk again. The most common form of rehabilitation of patients is through physiotherapy which dates back to 18th century. However, rehabilitation through electrical muscle stimulation surfaced in early 1960s. The advancements carried forward include the enhancement of the stimulation systems and patterns [2]. In 1986 electro-stimulation implants were developed and after several animal trials, these were successfully tested on humans [3]. Although there were various limitations associated with the electro-stimulation implants, still all of 4 patients who received these implants were able to walk again. A portable system for providing the stimulation patterns for walking was developed with a focus on the hardware implementation and inclusion of close loop control in stimulation as given in [4]. The tests were conducted on seven subjects which showed more flexible nature of the developed system as compared to earlier systems in terms of programming, memory capacity, and expanding user interface. Taking it a step further, a responsive electromyogram (EMG) based system for patient's intention detection has been developed [5]. The system is able to read the patterns of EMG signals from the upper trunk of the patient to activate the functional electrical stimulation (FES) for standing up and walking support. For standing of paraplegics, FES magnitudes need to be adjusted. Computer simulation based on the developed muscle activation models dictate the stimulation of the muscle and the feedback control law is developed to control the stimulation levels [6,7]. The effort towards gait rehabilitation using stimulation have also been surfaced in various forms [8,1]. The control of electrical stimulation for unsupported standing using the optimal scheme to optimize the amount of stimulation is studied [9,10]. The control of stimulation based on switching curve is given in [11].

* Corresponding author.
E-mail addresses: Ahmad.abdullah@mail.au.edu.pk (A. Abdullah), Zareena.kausar@mail.au.edu.pk (Z. Kausar), dramerhameed@gmail.com (A. Hameed), Shakilrs@mail.au.edu.pk (S.R. Shiekh), haroonkh@oslomet.no (H. Khan).

https://doi.org/10.1016/j.bspc.2021.102627
Received 30 June 2020; Received in revised form 9 September 2020; Accepted 5 April 2021
Available online 19 April 2021

Various other studies for standing, sitting and walking in paraplegics are given in [12–15]. Apart from FES being the key strategy for restoration of muscle activity in paraplegics, some model based approaches have also been studied in [16–21]. A combination of neuro-sliding mode control for FES was given in [22] which studied the development of a control strategy for better tracking of performance and for robustness against muscle joint dynamics. A different approach towards raising the standard of living of the paraplegic patients and enable them to perform their activities of daily living (ADL) is through the assistive devices. The studies on development of assistive devices have shown that the use of such devices raise the level of confidence among disabled persons [23–25]. These devices can be divided into two categories, first is exoskeletons and second is assistive platforms. The exoskeletons are wearable robots that assist the patient in standing up, sitting down and walking independently [26–30]. A detailed review of exoskeletons and their application in rehabilitation is given in [31]. There are few limitations associated with these exoskeletons regarding their daily life use and affordability. These include their bulkiness, weight, complexity and costs. The second approach focuses on the development of the mobile assistive devices keeping in mind patients who have complete disability in the lower region of their body. A novel approach towards the development of a rehabilitation platform for lower limbs has been presented in [32]. A wheel chair is the most obvious choice for an assistive platform for mobility of paraplegic patients. The design of a wheel chair is given in [33]. Various other commercially available standing wheel chairs such as Permobil® Corpus F5 provide various options and advantages over a normal wheel chair but the independence of the patient is still not ensured. The patient still needs an assistant to shift them from wheel chair to a bed or a chair and then back on to the wheel chair. To make paraplegic patients independent, the most important task is to enable them to sit and stand independently. A comprehensive study on the sit–stand (S-S) motion and its various parameters is presented in [34]. Dynamic programming is employed due to the complex nonlinear nature of the human bio-mechanic system. Optimal feedback control scheme is used to find a compromise between human balance and smoothness of motion and its control constraints. The human motion is modeled using a device for performing sit–stand motion and collection of data. Another similar device intended for transferring the patient from one platform to another is proposed and evaluated by Hari Krishnan and Pugazhenthi [35]. The device is intended for transfer of a paraplegic patient from wheel chair to toilet seat or chair with any help from an assistant.

Most of the devices under discussion are of non-linear nature due to complexity in their design and presence of coupling and uncertainties in the system. In all of the studies mentioned above, control has been an essential part of every effort as it ensures reliable and responsive behavior of the system. Studies [29,36–38] show that a responsive and reliable control scheme is the key to success for rehabilitation devices. A modular PD-fuzzy control for Sit to stand and stand to sit motion control for upright standing of two wheeled wheel chair is presented in [38]. The device depicts an inverted pendulum which is an example of a complex system. PD scheme along with fuzzy controller is implemented in order to achieve the upright standing and movement of the wheel chair. A combination of sliding mode and fuzzy control is presented in [36]. The combination is proposed in order to realize independent joint control based on the complex nueromusculoskeletal dynamics, disturbances and other dynamics related changes in the system. In addition to a control scheme, the use of muscle/brain signals for activation/deactivation of such devices is also gaining popularity and its effectiveness for the activation of robotic devices is well established now a days. Various studies are available in literature which demonstrate the use of biological signals for intention detection as well activation/de-activation of robotic devices. Such techniques increase the flexibility and ease of use of an assistive device for patients with disabilities. A detailed review of various steps involved and various types of biological signals that are used to interface the human body with a robotic device is presented in [39]. A closed loop system based on neurofuzzy control and extended physiological proprioceptive feedback provides a means for bidirectional control of an exoskeleton [40]. EMG signals from muscles are acquired and used for intention detection and for activation of control loop which actuates the exoskeleton. Another study showing the applicability of bio signals for activation of robotics devices is presented in [41]. A mobile robot and a serial manipulator are controlled using EMG and EEG signals acquired from human muscle and brain respectively. An EEG-NIRs based alternative to more popular approaches of EEG and EMG signals is used in the study [42]. Near infrared spectroscopy is an optical signal based approach for signal acquisition while EMG and EEG are both electrical signals generated in brain. In this study, EEG-NIRs based intention detection system is developed for control of assistive devices. Another integration of EEG based human machine interface (HMI) for activation of an assistive device controlled by neural adaptive sliding mode control is proposed. The integrated framework is tested on an upper limb exoskeleton [43]. The scheme used shows that effectiveness of an assistive device is enhanced by integration of a HMI based activation system integrated with a robust nonlinear controller. The assistive devices such as exoskeletons and other similar devices aimed for rehabilitation have a complex mechanical structure due to their design constraints. Moreover, the complexity of design gives rise to many challenges in reliable and smooth control of such devices due to their nonlinear dynamics models. To cater for these non-linearities, many of the studies mentioned above use a combination of two or more control schemes such as, Adaptive Sliding Mode Control, Adaptive Neural fuzzy control and fuzzy sliding mode control etc. Sliding Mode control has been widely used for system which have non-linearity and uncertainty in their models [44].

Based on the above discussion on the combination of bio signal acquisition for intention detection for activation of a robotic device having its dedicated control system, a rehabilitation device is presented in this study which uses EEG signals for acquisition of patient's intention and activation of control system on board the device. EEG signals are selected due its ease in practical implementation and high temporal resolution. Further details about EEG are discussed in the next section of this paper. In this study a device for independent sit–stand (S-S) motion for paraplegic patients is presented. The intention of patient is acquired using EEG signals from eye blinks which in turn activate the control system to actuate the device from Sit to Stand position or vice versa. The platform is designed keeping in mind the independence and mobility requirements of paraplegic patients. For control of S-S motion, two types of control schemes: linear and nonlinear, are proposed namely proportional integral derivative (PID) control and sliding mode control (SMC). PID is a well-known technique for various robotic systems and thus is chosen here as a default control scheme whereas SMC is non-linear control technique and is chosen due to its properties of stability and robustness against disturbances and non-linearities of the system. The choice of a nonlinear control system is made because the S-S mechanism Model is nonlinear itself. The experimental setup consists of a Subject wearing EEG headset. The intention detection system detects the intention of patient through HMI framework which generates control commands in the results of an intention, i.e. eye blinks. The control commands are then used to activate the control system which in turn actuates the S-S mechanism. The system description in image form is shown in Fig. 1.

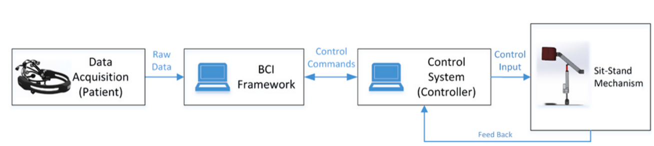

Fig. 1. System block diagram.

2. Intention detection

Human machine interface (HMI) is required in various conditions. For example, if a patient is supporting him/herself on the platform using upper limbs then he cannot press a button or move a joystick. In that condition an alternative way must be provided for the patient to convey his/her intention to the machine. Therefore, the use of brain signals or Muscle signals becomes significant. The intention of patient, in this study, was detected using EEG signals from eye blinks which were then processed for acquiring the intention of the patient and generating control commands as shown in Fig. 2.

EEG is the electric potential created due to brain activity [45]. Usually ranging around 100 μV, it can be acquired directly from the scalp. This technology is comparatively less expensive and provide more flexible data acquisition. One of the major advantage of using EEG signals was that it has good temporal resolution [42].

2.1. Data acquisition

EEG data was collected non-invasively, using small gold plate electrodes. A basic EEG system includes: electrodes, amplifiers with filters, an analog-to-digital converter, and a recording device for the storage of data. The intensity of the electrical source, its distance from the recording electrodes, its spatial orientation, and the electrical properties of the structures between the source and the recording electrode all play a role in determining the amplitude of the recorded potentials. The EEG equipment, therefore, used in this study was the EMOTIV® EPOCH^{+} which is a 14 channel wireless EEG headset designed for advance HMI interface applications. It provides dense array high quality raw EEG data. EMOTIV® EPOCH^{+} has 14 EEG channels along with 2 reference channels [46]. The intention of the patient is recorded in this study using eye blink signals.

2.1.1. Experimental paradigm

In this study, five healthy individual with ages between 25 and 30 years were selected for the experiment. Each experiment consisted of 5 trials. The subjects were seated in a calm and comfortable environment. Each subject was given 15 min before the start of experiment to practice the task and to get used to EMOTIV® EPOCH^{+} headset. The subjects were asked to focus and concentrate on eye blinking. Each subject was provided auditory cues of “rest” and “blink”. The data was taken from 5 healthy subjects. The total duration of the paradigm was 12 s excluding the initial 2 s intervals before each run. A visual representation of the experimental paradigm is shown in Fig. 3.

2.1.2. Pre-processing

There are various artefacts in the EEG signals that need to be removed. One of these artefacts is the EMG component present in EEG signal. Since voluntary eye blinks are considered as intention in this study, Therefore the EMG component for eye blinks is not taken as artefact [47]. In fact, the EMG component present in EEG signal is useful and can be treated as a parameter for better detection of eye blinks. In the present study, the prepossessing step was performed on a tool box named EEGLAB [48] developed by Swartz Center for Computational Neuroscience, University of California, San Diego. The raw data acquired using headset was passed through a band pass Finite Impulse Response (FIR) filter which is given by Eq. (1). The cut off frequency used for FIR band pass filter was 04–25 Hz:

$$y[n] = \sum_{k=0}^{M} [b_k x[n-k]] \tag{1}$$

where M is the order of the filter, $y[n]$ is the output signal, $x[n]$ is the input signal and b_k contains filter coefficients.

2.1.3. Feature extraction

Feature extraction step decides the criteria on which the data is going to be classified. The difference between various statistical features helps in sorting the data into group correctly. Five features calculated for the filtered signal in this study were mean, peak, variance, kurtosis, skewness and slope. The formulae for these features are given in Table 1.

2.1.4. Classification

LDA (linear discriminate analysis) developed by Fisher is one of the most common technique used to classify data. It is very effective in classification of binary as well as in more than two class problems [49]. But its effectiveness reduces as number of classes increase and therefore for multi class problems, other classifiers are also available. Fisher linear discriminant analysis (FLDA) reduces the dimension of the problem by one degree and finds a line that best separates the classes in a two class problem. Similar analogy is followed for more than two classes but the accuracies drop significantly for more than two class problems. The

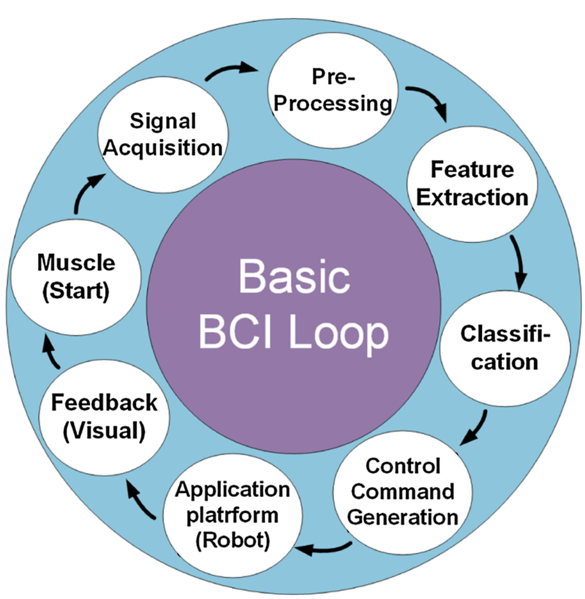

Fig. 2. Intention detection and command generation loop.

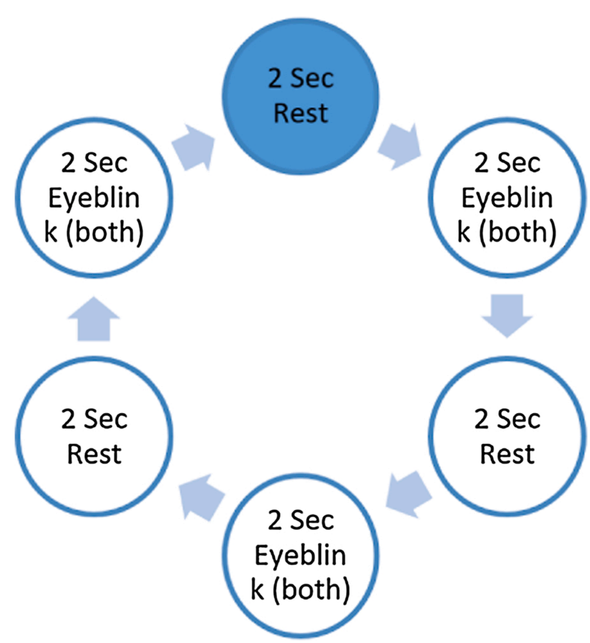

Fig. 3. Experimental paradigm.

Table 1
Selected features.

Feature	Formula
Mean	$M = \frac{1}{N}\sum_{i=1}^{N} X_i$
Variance	$V = \frac{1}{N-1}\sum_{i=1}^{N} \lvert X_i - \mu^2 \rvert$
Kurtosis	$K = \frac{E(X-\mu)^4}{\sigma^4}$
Skewness	$S = \frac{E(X-\mu)^3}{\sigma^3}$

classification accuracies are computed for various combination of features. Among them, features that gave the best accuracies using FLDA are given in Table 2.

2.2. Control command generation

The correct identification of the class ensures that the classifier will classify the incoming data correctly. The data from each subject was tested against the training data. Each class is assigned a letter for example, for rest "u" is assigned whereas for blinking the assigned letter is "v". Each time the test data is checked against the training data, the classifier identifies to which class that data belongs to. If the class is identified as "v", an actuation command is generated which actuates the S-S mechanism. otherwise the mechanism remains at rest. This command then activates the control algorithm and S-S Mechanism which complete its motion from sit to stand position at each command and then waits for the next command.

3. The S-S mechanism: description and modeling

The assistive device for paraplegics is a platform that is designed for active daily life (ADL) tasks as well as for therapy purposes. It facilitates the patient in being independent and perform their small endeavors themselves.

3.1. Description

The device offers the S-S motion as well as mobility to the patients using it. This study focuses on the design and dynamics of the S-S mechanism. The device is designed keeping in mind the common needs and the comfort of patient. The ease of use is one of key factors in proving effectiveness of the device.

The device in discussion has two main parts. First is the S-S mechanism which is under discussion in this study, and the other is the mobile platform which will be discussed in the upcoming publications. The physical prototype of the device can be seen in Fig. 4. The S-S mechanism consists of two revolute joints and one prismatic joint. The prismatic joint is actuated using a linear actuator. The extension and retraction of linear actuator moves the end effector which in turn moves the patient from sitting position to standing or vice versa. To find out the required torques and to analyze the dynamic response of the system, modeling and control of the system is discussed in upcoming section of this study.

Table 2
Classification accuracy.

Subject	Mean, peak, slope, variance, kurtosis, skewness	Mean, kurtosis, skewness	Variance, kurtosis
1	85.94	83.59	83.98
2	88.09	82.81	82.21
3	87.13	80.02	82.03
4	87.89	80.08	80.06
5	83.98	79.99	80.06

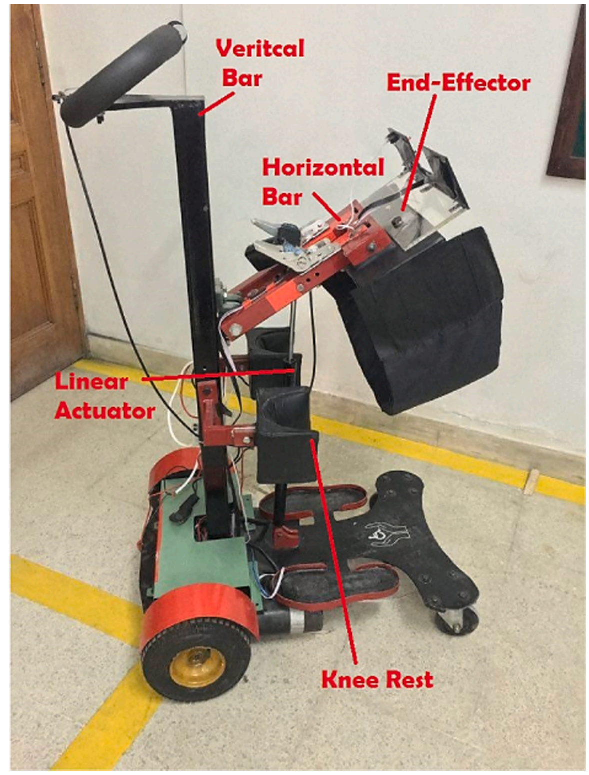

Fig. 4. Paraplegic bot prototype at Air University.

3.2. Dynamics modeling

For dynamics modeling of the S-S mechanism, the Euler Lagrange method is adopted. The S-S mechanism has been considered as RPR (Revolute–Prismatic–Revolute) mechanism having a revolute joint followed by a prismatic and then again a revolute joint. The kinetic and potential energy of each link is considered for Euler–Lagrange formulation.

The free body diagram is shown in Fig. 5. The two revolute joints of the S-S mechanism are passive while the prismatic joint is actuated by a linear actuator.

Lagrangian is the sum of total kinetic energy and potential energy of the system. The kinetic energy equation is written for each link using Eq. (2), where $i = 1, 2, 3$:

$$k_i = \frac{1}{2} m_i {V_{C_i}}^T V_{C_i} + \frac{1}{2} {}^{i}_{i}\omega^T \, {}^{C_i}_{i}I \, {}^{i}_{i}\omega \tag{2}$$

The sum of the total kinetic energy for three links can be given as Eq. (3):

$$K = \sum_{i=1}^{3} k_i \tag{3}$$

Similarly, the sum of potential energy for all the links can be given using Eqs. (4) and (5):

$$u_i = m_i l_i g S_i + m_i l_i g \tag{4}$$

$$U = \sum_{i=1}^{3} u_i \tag{5}$$

In Eqs. (2)–(4) m_i is the mass of ith link, l_i is the length of ith link, g is acceleration due to gravity, S_i represents $[\sin(\theta_i)]$, V is linear velocity and ω is angular velocity for ith link. Finally, to compute the equations of motion, the Lagrangian was computed which is given as Eqs. (6) and (7):

$$L(\Theta, \dot{\Theta}) = K(\Theta, \dot{\Theta}) - L(\Theta) \tag{6}$$

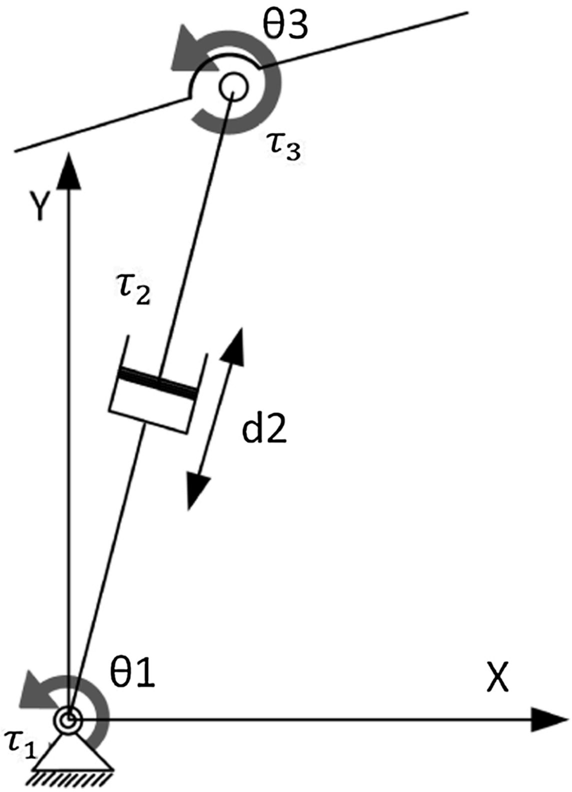

Fig. 5. Free body diagram of S-S mechanism.

$$\frac{\mathrm{d}}{\mathrm{d}t}\frac{\partial L}{\partial \dot{\Theta}} - \frac{\partial L}{\partial \Theta} = \tau \tag{7}$$

which is equivalent to Eq. (8):

$$\frac{\mathrm{d}}{\mathrm{d}t}\frac{\partial K}{\partial \dot{\Theta}} - \frac{\partial K}{\partial \Theta} + \frac{\partial U}{\partial \Theta} = \tau \tag{8}$$

After manipulation of the above equations we arrived at the results given in Eqs. (9)–(11):

$$\tau_1 = (m_1 l_1^2 + +\mathrm{Izz}_1 + m_2 d_2^2 + \mathrm{Iyy}_2 + m_3 l_{c_3}^2 + \mathrm{Ixx}_3 S_3^2 + \mathrm{Iyy}_3 C_3^2)\ddot{\theta}_1 + 2m_2 d_2 \dot{d}_2 \dot{\theta}_1 - m_2 d_2 \dot{\theta}_1^{\,2} + (m_1 l_1 + m_2 d_2)\mathrm{g}\mathrm{C}_1 + m_3 \mathrm{g} l_{c_3}(S_1 S_3 - C_1 C_3) \tag{9}$$

$$\tau_2 = (m_2 + m_3)\ddot{d}_2 - m_2 d_2 \dot{\theta}_1^{\,2} + m_2 g S_1 \tag{10}$$

$$\tau_3 = (m_3 + \mathrm{Izz}_3)\ddot{\theta}_3 - (\mathrm{Ixx}_3 S_3 C_3 - \mathrm{Iyy}_3 C_3 S_3)\dot{\theta}_1^{\,2} + m_3 g l_{C_3}(C_1 C_3 - S_1 S_3) \tag{11}$$

where τ_i is the torque produced at ith joint, d_2 is displacement of linear actuator, C_i, S_i are $\cos(\theta_i)$, $\sin(\theta_i)$, m_i is mass of the ith link, I moment of inertia of the ith link along respective axis and l is the length of ith link. Link-1 is actuated by first revolute joint, link-2 is actuated by the prismatic joint and link-3 by the second revolute joint. The parameters like mass and moment of inertia were computed from the 3D CAD model by assigning a material to the model. The link lengths were taken from the actual system.

4. Control of S-S mechanism

The purpose of the assistive device is to assist the patient in sit to stand motion. Therefore, it is of key importance that the control of the S-S mechanism must be very reliable. Also it is evident from the equations of motion that the system is highly non-linear, thus a suitable control strategy is required in order to control the system using minimum computational as well as energy cost. This work is intended to provide a comparison between two of the popular control techniques. For practical Systems, the requirement of control scheme to be applicable on physical system is imperative. For industrial systems, PID is the first choice as a control scheme due to its versatility and application. Therefore, PID was chosen for the control of the assistive device. While, SMC belongs to the family of variable structure controllers (VSC) which change the structure of the controller according to changing system dynamics. SMC among VSC's was found to be more suitable for practical application due to simplicity in its design and performance. The intention was to show case the effectiveness of the chosen control schemes under given circumstances. The same model was given to both the control system and their response was simulated using Matlab® Simulink®. The desired value for both the simulation as well as experimental setup was kept equal to 0.2 m or 20 cm. This is the desired displacement of linear actuator for it to reach from sitting position to standing position and vice versa. The speed of the S-S mechanism is acquired by calculating the time required for a normal human being to stand up from sitting position and vice versa.

4.1. Proportional integral derivative (PID) controller

PID control is among the popular control techniques and has proven its effectiveness in various fields including biological systems as well. In this study, PID control strategy is applied for the control of S-S mechanism to control its position and velocity. The simplicity of the PID makes it the first choice among the control techniques. The motion of the S-S mechanism needs to be controlled for smooth movement from sitting to standing position and vice versa. The control cost needs also to be kept within the range of physically possible and available actuator torques since the actuator is required to support the weight of human being while moving the mechanism between sit and stand positions.

The PID controller also known as a three term controller has various forms. In this study, the standard form of PID is used which is given as Eqs. (12) and (13). Where e is the error, k_p is the proportional gain, k_i is the integral gain and k_d is the derivative term gain

$$u = k_p e + k_i \int_0^t e(\tau)d\tau + k_d \frac{\mathrm{d}e}{\mathrm{d}\tau} \tag{12}$$

$$u = k_p(e + \frac{1}{T_i}\int_0^t e(\tau)d\tau + T_d \frac{\mathrm{d}e}{\mathrm{d}\tau} \tag{13}$$

Table 3
PID parameters and their relations.

Gain	Rise time	Overshoot	Settling time	Steady state error	Stability
K_p	Decrease	Increase	Small change	Decrease	Decrease
K_i	Decrease	Increase	Increase	Eliminate	Decrease
K_d	Small change	Decrease	Decrease	No effect	Improve if K_d is small

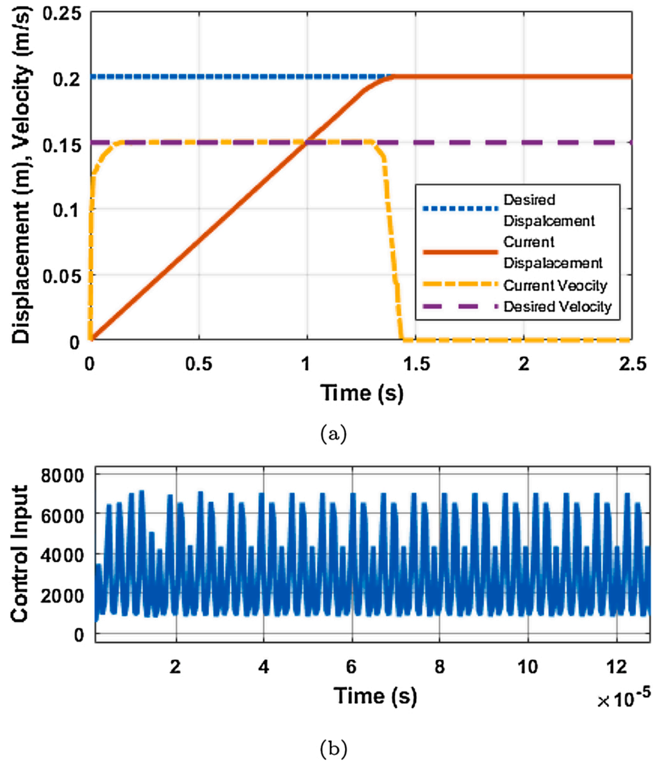

Fig. 6. Simulation results for PID control, (a) displacement–velocity plot and (b) control input/controller effort required.

The relationship between the three terms in the PID controller cannot be stated exactly but an overview of the effects of each term on output can be given as Table 3. The tuning of PID controller is a crucial and essential part of the controller implementation. In literature, there are various methods available for calculating the appropriate gains for the controller. In this study we have used the Ziegler–Nicholas method for PID gain tuning. The PID implementation in this study includes the combination of the position and velocity control for the S-S mechanism. Two PID controls are used in conjunction to achieve better control for both velocity and position. The non-linearity in the system brings uncertainty in the behavior of the system and thus a more robust control is required for both velocity and position. It can also be seen from the results shown in Fig. 6 that the system requires a huge control effort in order to bring the system to the desired position.

After simulating the system under various conditions for desired response, it was observed that the magnitude of the torque requirement for the system is very high and also that it leaves the physical bounds of any actuator to fulfil it. The control requirement is high due to the non-linearities present in the system. The behavior of the system is very sensitive to inherent and external disturbances caused by the fluctuation of gains or by changing the input conditions. The PID controller toolbox in Simulink® also has an auto-tuner function. The auto tuning of the PID control also exhibited the same response. The input torque requirement to control the system are the same for auto tuning as for the manual tuning. Further discussion and comparison of the results in the results and discussion section of this study.

4.2. Sliding mode control

Sliding mode control belongs to a family of control strategies known as variable structure control (VSC). This family of controller provides a good variety of robust control techniques and methods. This is mainly the motivation behind selection of the sliding mode control. The non-linear and time varying characteristics of the system and the absence of a precise model of the system urges the need for a control strategy such as sliding mode control.

4.2.1. Design of sliding mode control

The selection of a suitable sliding manifold is the key component of the sliding mode control. This manifold acts as a guide for the system states to track along it to reach the desired value. The design of the sliding manifold is based on system requirements. In this study, it is desired that the position error must be zero. We defined the current and desired position as x and x_d as in Eqs. (14) and (15):

$$x = [x, \dot{x}, \dots, x^{n-1}] \tag{14}$$

$$x_d = [x_d, \dot{x}_d, \dots, x_d^{n-1}] \tag{15}$$

Therefore, we write the error as Eq. (16)

$$\tilde{x} = x - x_d \tag{16}$$

We defined a time varying 1st order sliding manifold given in Eq. (17) since the system is of 2nd order

$$s(x,t) = \left(\frac{\mathrm{d}}{\mathrm{d}t} + \lambda\right)^{n-1} \tilde{x} = 0 \tag{17}$$

which is rewritten as Eq. (18)

$$s(x,t) = \dot{\tilde{x}} + \lambda \tilde{x} = 0 \tag{18}$$

where n is the order of the equation and λ is a constant gain.

4.2.2. Design of control law

The control law design based on the sliding manifold requires the stability of the sliding manifold itself as well. We design the control by solving Eq. (18) to get an equation for equivalent control. The system dynamics while the system is on sliding surface can be given by Eq. (19):

$$\dot{s} = 0 \tag{19}$$

This equivalent control is responsible for keeping the system on sliding surface. It can only be assured if the product of sliding surface s with its derivative $\dot{s}$ is less than zero and Eq. (19) remains satisfied. If the sliding surface satisfies the above condition, then we can say that sliding manifold is stable and the system states will converge to the desired value under the equivalent control. Thus we write the derivative as Eqs. (20) and (21):

$$\dot{s} = \ddot{\tilde{x}} + \lambda \dot{\tilde{x}} \tag{20}$$

$$\dot{s} = \ddot{x} - \ddot{x}_d + \lambda \dot{\tilde{x}} \tag{21}$$

The control law for SMC has two parts as given in (22). The first part is the equivalent control while the other is the corrective control. The equivalent control is responsible for bringing the system on the sliding surface and the corrective part is responsible for keeping it there:

$$U = U_{eq} - U_c \tag{22}$$

Setting $\dot{s} = 0$ and substituting $\ddot{d}_2$ in equation, we arrive at the result for the best approximation for equivalent control Eq. (23):

$$\hat{U} = (m_2 + m_3)\ddot{\tilde{x}}_d - \lambda \dot{\tilde{x}}(m_2 + m_3) - m_2 d_2 \dot{\theta}_1^{\,2} + m_2 g sin\theta_1 \tag{23}$$

where $\hat{U}$ is interpreted as the best approximation of equivalent control. Keeping in mind the uncertainty of dynamics, we added another discontinuity to $\hat{U}$ to ensure that the condition for the stability is satisfied which resulted in the control law given in Eq. (24):

$$U = \hat{U} - \mathrm{ksgn}(s) \tag{24}$$

In Eq. (24), k is chosen large enough such that the reachability condition is satisfied. The reachability condition is given as Eq. (25):

$$\frac{1}{2}\left(\frac{\mathrm{d}}{\mathrm{d}t}\right)s^2 \leq -\eta|s| \tag{25}$$

where η is a positive gain. It can also be stated alternatively as Eq. (27). The reachability condition is only satisfied when both the control law and the sliding surface are stable. To ensure the stability we use Lyapunov stability criteria considering a positive scalar function V as the candidate function as given in Eq. (26):

$$V = s^2 \tag{26}$$

The derivative of the scalar function V must be negative definite in order for the sliding surface and the control law to be stable over the whole range of operations. Therefore the condition given in Eq. (27) must remain true for the complete range of operation:

$$\dot{V} = s\dot{s} < 0 \tag{27}$$

By manipulating Eqs. (23) and (24) to satisfy the condition in Eq. (27), we arrive at Eq. (28).

$$s\dot{s} = \left(\frac{1}{m_2 + m_3}[-\mathrm{ksgn}(s)]\right)s \tag{28}$$

Eq. (28) shows that if gain k is chosen carefully then the overall sign of the above equation remains negative at all times which proves that the reachability condition exists for the system under study. Eq. (24) is the control law which will control the system within the bounds of operation. To illustrate the implementation of the control law, the simulation results are shown in Fig. 7. Similar to PID simulations, the simulation results are obtained after implementing SMC in Simulink® environment. SMC gains were tuned to acquire the best possible results. Simulation results show that SMC performs better than PID.

One of the main issues associated with the sliding mode control, as evident from the results shown in Fig. 7, is the problem of chattering in the system. A few attempts on avoiding chattering phenomenon to improve the performance of the controller are given in [36,50,51] which discuss the ability of the controller to handle uncertainties of the system while keeping the system and controller itself stable. The initial implementation of the sliding mode controller resulted in chattering as shown. The chattering issue is due to the sign function in the control law. The implementation of control switching is imperfect, as in practice, the control switching is not instantaneous and thus it leads to chattering. In

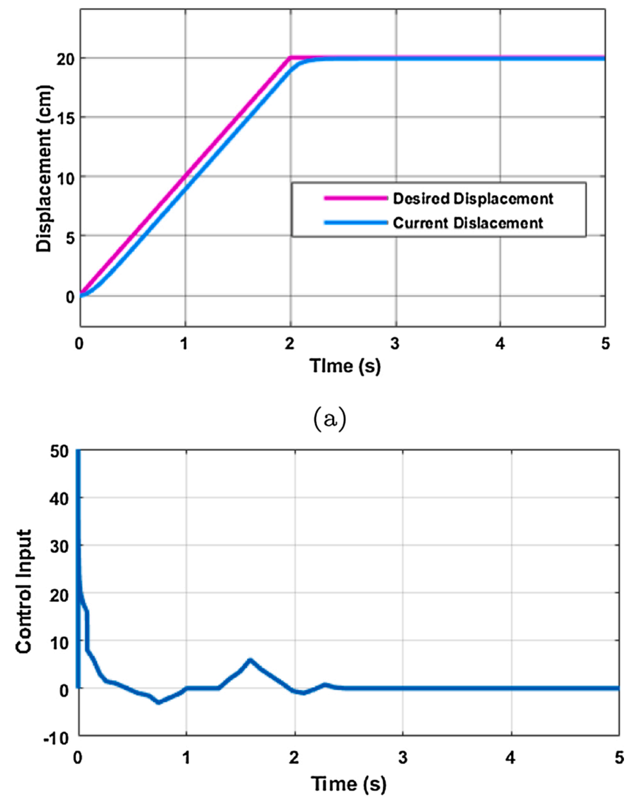

Fig. 8. Simulation results for sliding mode control without chattering, (a) displacement plot, (b) control input.

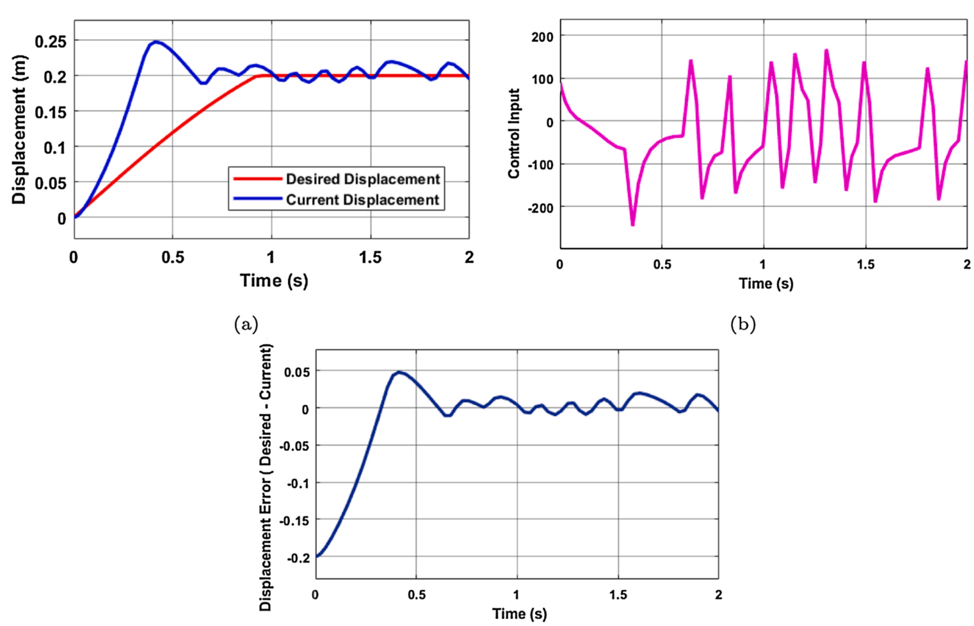

Fig. 7. Simulation results for sliding mode control with chattering, (a) displacement plot, (b) control input and (c) error plot.

order to eliminate the undesirable effect of chattering from the response, we define a boundary layer around the switching surface. The purpose of the boundary layer is to keep the system on the switching surface as the control law forces the system to remain within the boundary layer. The implementation of such control law also makes the controller robust against the unwanted high frequency dynamics. The boundary layer was defined as Eq. (29):

$$B(t) = x, |s(x,t)| < \phi \quad \text{for} \quad \phi > 0 \tag{29}$$

The updated control law can now be given as Eq. (30):

$$u = u_{eq} - \mathrm{ksat}(s\phi) \tag{30}$$

The results obtained after the implementation of the updated control law are shown in Fig. 8.

5. Experimental results

The experimental results are acquired using the prototype of the device developed at the Department of Mechatronics Engineering, Air University. The experimental setup consisted of device prototype, a PC running Matlab®. Simulink® and EEG headset. S-S mechanism of the assistive device enables the patient to strap himself to the mechanism and the linear actuator then actuates the mechanism according to generated commands. The EEG headset acquires eye blink signals and the PC generates control commands after classification. The device and EEG headset are both connected to the PC where the control algorithm is running after taking inputs from both the EEG headset and device prototype. An illustration of S-S mechanism while it is in motion is shown in Fig. 9. In Fig. 9, (a)–(d) illustrate motion from sitting position to standing position and (d)–(a) show the motion from standing position to sitting position. Two subjects voluntarily participated in experimental trials of the proposed device prototype. The EEG data was taken from both the subjects for training of the classifier and for generation of control commands. Patient comfort and confidence on the proposed device was ensured. To ensure comfort during motion during motion, both the PID and SMC control schemes are implemented on the prototype and the results are obtained. The results are presented in this section and further discussion is given in the next section of this paper.

For acquiring the experimental results, the complete setup was established as shown in Fig. 9. A healthy subject wearing the EEG headset was strapped to the sit–stand mechanism of the assistive device prototype. The experiment was performed in a calm environment, with all the precautionary measures, after taking consent of the subject. The subject was carefully strapped to the device such that the weight of the whole body was supported by the sit stand mechanism while in operation. The subject was asked to blink 5 times in order to activate the device. EMOTIV® EPOCH$^+$ headset was wirelessly connected to a PC running Matlab® for classification of the incoming data.

After classification, the control commands were generated which then activated the sit–stand mechanism. The sit-stand mechanism is powered by its own AVR based embedded system. This enabled the connection between sit–stand mechanism and a PC running hardware in loop simulation. The control scheme was implemented in Simulink® environment on Matlab®. The sensor feedback from the sit stand mechanism was fed to the Simulink® environment for control implementation and the control input was in return fed to the sit stand mechanism. The complete experimental setup is illustrated in a block diagram in Fig. 10.

First, the PID control scheme was tested. The results were similar to those in simulation. PID control was not able to control the physical system with the imposition of a saturation function. For tuning of the PID controller, initially, the three gains producing best results in simulation of the controller were selected. The response of the system indicated high amplitude oscillations which showed that the controller needed further tuning. After rigorous tuning the best results obtained for a PID controller are shown in Fig. 11. The response is not satisfactory and needs further refinement. The response shown is tuned for very high values of P, I and D gains which translated into very high control input. The gains of the terms were so high that the PWM driving the actuator always remained full and it was not feasible. The high speed and sudden motion of the mechanism made the subject uncomfortable. Additionally, it is not able to hold the system under control. System remained fluctuating when it reached near to its desired point. The PID control was not able to keep the system exactly on the desired position. This continuous oscillation of the system is not feasible for an actual actuator as it may become the cause of failure of the actuator itself. The continuous oscillation was also harmful for the mechanical structure of the device. This also created a limitation for the linear actuator due to it continuous energization and operation. Thus the experimental results verified the simulation results. It can be clearly seen in the Fig. 11 that the controller is not able to control the system even after the implementation of a saturation function on values of control input. The saturation was applied to prevent any damage to the system in case of high amplitude spikes in the control input which were seen during the tuning of PID controller.

The simulation results for SMC showed that it can control the system. After PID, SMC was implemented on the system. SMC is a non-linear control scheme having robust properties which makes it ideal for non-linear systems. Simulation results have already shown that SMC was able to control the system under study. The experimental results were acquired using the same setup as used for PID control tests. The desired

(a) **(b)** **(c)** **(d)**

Fig. 9. Illustration of sit to stand and stand to sit motion.

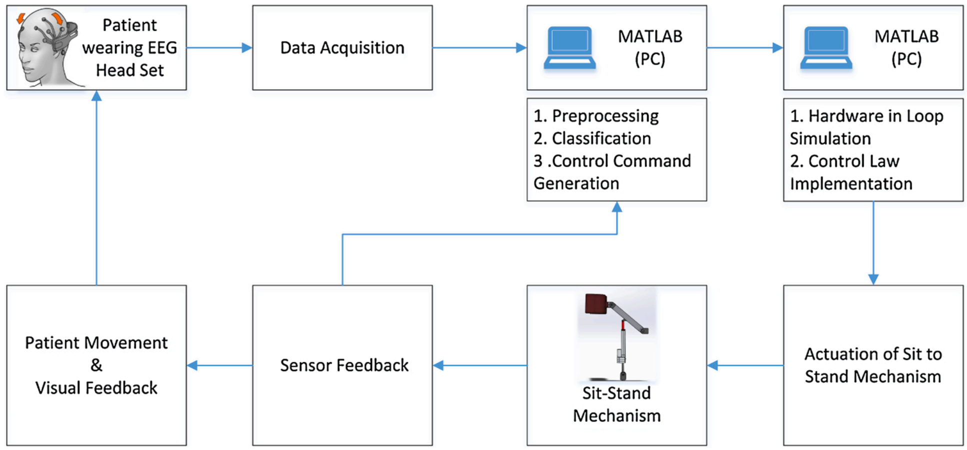

Fig. 10. Block diagram for experimental setup for S-S mechanism including EEG headset.

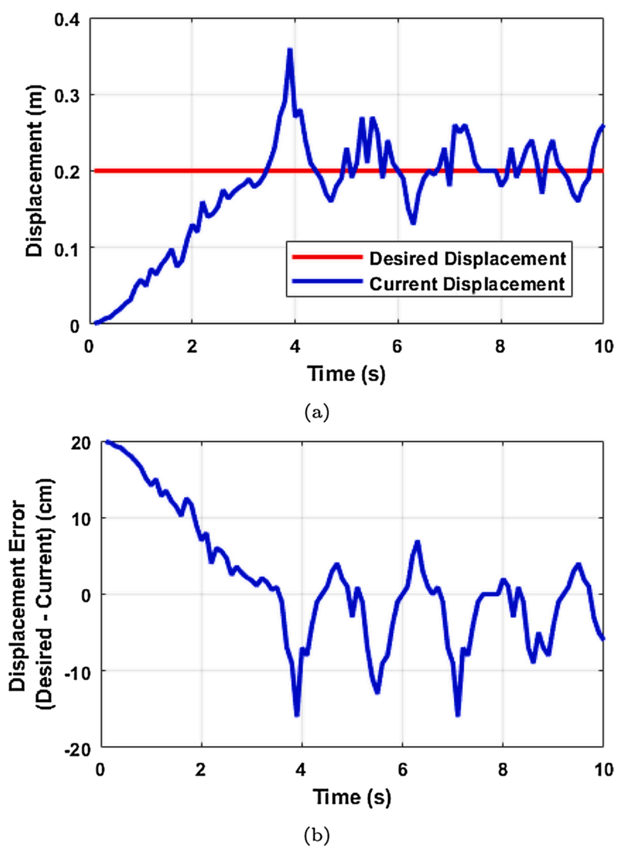

Fig. 11. Experimental results for PID, (a) displacement plot and (b) error plot.

point and the actuation setup was the same as used in previous tests. Similar to PID control scheme, SMC control scheme also needed tuning. SMC controller has two terms λ and k as gains for tuning the controller. These two gains determine the response of the controller and system. The results obtained after tuning these two parameters are shown in Fig. 12.

6. Discussion

A suitable controller is the key to better performance and long life for a system that is to be used on daily basis by a patient to fulfil his ADL tasks. The purpose of this research was to present a study on modeling and control of the device that is intended to be used by disabled patients for the purpose of sit-stand motion. The main control problem identified in the system under study was the non-linear nature of the system itself. The non-linearity of the system is evident from its equations of motion as well as its behavior as shown in Figs. 6 and 7. The simulation results were obtained for the two control schemes selected. The results of the PID controller indicate that the controller requires a great effort in order to bring the system under control. This was due to the high values of the P, I and D gains. The change in dynamics of the system due to change in posture of the patient during sit to stand motion produces oscillation in the system which could not be rejected by PID controller as evident in Fig. 11. Such huge values of control input are not realizable by an actuator. Thus it becomes inevitable to limit the value of control input to a feasible region. It is also evident from comparison of simulation and experimental results shown in Figs. 6 and 11. The system response for both simulation and experimental setup show that PID controller is not sufficient for the system under study. Therefore, we needed a more advanced non- linear controller in order to bring the system under control. SMC is a type of control scheme that embodies two very useful aspects. One is its non-linear nature which it inherits from its family of variable structure control schemes. The other aspect is the in-variance to the parameters of the system which makes it a robust controller. Combining these aspects together, most of the non-linear systems can be controlled. Another aspect of SMC which enhances its feasibility and application on various types of non-linear systems is the design of the sliding surface. For more complex systems, more complex sliding surface is used. However, for the proposed system we used first order sliding surface. The SMC performed better as expected both in simulation and experimental evaluation which is evident from Figs. 8 and 12. One of the challenges in implementation of SMC was the tuning of gains. It is important to understand the impact of each gain on system response and the relationship of the two gains with each other. The fine tuning of these gains produces fine results which can be seen in Fig. 12.

7. Conclusion

For rehabilitation and assistive devices, the level of concern for a good design and suitable control shames is inevitable. It is also very important to provide a suitable interface through which the user can interact with the device. In this study, we proposed an EEG based human machine interface for the actuation of the device, the model of an assistive device and a comparison between two control schemes for the control of states of S-S mechanism of the proposed assistive device. The device prototype was developed and experimental testing was performed based on an offline human machine interface. EEG signals from eye blinks were taken and classified for generation of control commands which triggered the system with 88% accuracy. The SMC scheme was found effective in controlling the S-S mechanism of the device under

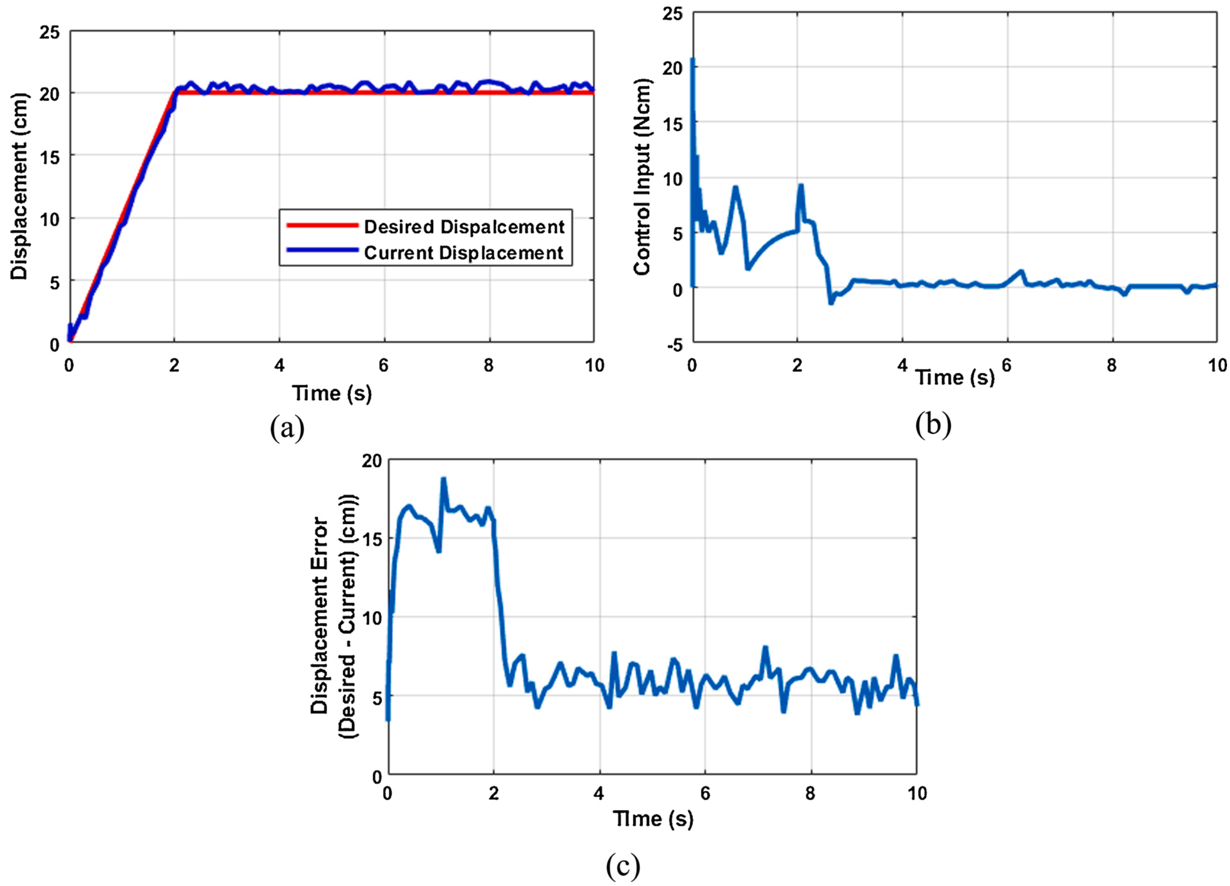

Fig. 12. Experimental results after SMC implementation, (a) displacement plot, (b) control input plot and (c) error plot.

study. With SMC scheme, the system required significantly less control effort and produced robust results as compare to PID. However, further experimentation is required to improve the response and thus the performance of the device. In future version of this work, we intend to apply a hybrid controller for further enhancing the performance of SMC and improving the performance of the S-S system. It is also intended that a dedicated embedded system be installed in the device for online classification of EEG signals and running the control algorithm on board the device.

Authors' contribution

Ahmad Abdullah: methodology, software, validation, formal analysis, investigation, resources, data curation, writing-original draft, visualization. Zareena Kausar: conceptualization, methodology, resources, supervision, project management, funding acquisition, writing-review. Aamer Hameed: conceptualization, methodology, resources, writing-review, investigation. Shakil Rehman: resources, writing-review. Haroon Khan: software, investigation, resources, formal analysis, writing-review & editing, funding.

Acknowledgments

This project is a joint venture by Higher Education Commission of Pakistan and Department of Mechatronics and Biomedical Engineering (DMBE) at Air University. The Project is financially supported by Higher Education Commission of Pakistan under the Technology Development Fund 2018 (Grant number: TDF02-223). The funding covers development, commercialization of the project and its legal affairs. DMBE initiated this project and developed the mathematical Model and prototype for the system. We are thankful to all the subjects who volunteered for EEG data collection and device testing. The ethical approval for these tests was taken from the ethical committee of Air University. The equipment and software used for this work are licensed versions in the name of Air University. The authors would also like to thank the faculty of Technology, Art and Design, OsloMet, Norway for making this collaboration possible.

Declaration of Competing Interest

The authors report no declarations of interest.

References

[1] R. Kobetic, E.B. Marsolais, Synthesis of paraplegic gait with multichannel functional neuromuscular stimulation, IEEE Trans. Rehabil. Eng. 2 (2) (1994) 66–79.

[2] W. Liberson, Functional electrotherapy: stimulation of the peroneal nerve synchronized with the swing phase of the gait of hemiplegic patients, Arch. Phys. Med. 42 (1961) 101–105.

[3] H.G. Stoehr, J. Holle, E.A. Kern, Application of gate arrays in implants for nerve stimulation (remobilization of paraplegic patients), IEEE Trans. Ind. Electron. 4 (1986) 361–365.

[4] G. Borges, K. Ferguson, R. Kobetic, Development and operation of portable and laboratory electrical stimulation systems for walking in paraplegic subjects, IEEE Trans. Biomed. Eng. 36 (7) (1989) 798–801.

[5] D. Graupe, Emg pattern analysis for patient-responsive control of fes in paraplegics for walker-supported walking, IEEE Trans. Biomed. Eng. 36 (7) (1989) 711–719.

[6] G. Khang, F. Zajac, Paraplegic standing controlled by functional neuromuscular stimulation. I. computer model and control-system design, IEEE Trans. Biomed. Eng. 36 (9) (1989) 873–884.

[7] G. Khang, F.E. Zajac, Paraplegic standing controlled by functional neuromuscular stimulation. II. computer simulation studies, IEEE Trans. Biomed. Eng. 36 (9) (1989) 885–894.

[8] G.T. Yamaguchi, F.E. Zajac, Restoring unassisted natural gait to paraplegics via functional neuromuscular stimulation: a computer simulation study, IEEE Trans. Biomed. Eng. 37 (9) (1990) 886–902.

[9] K.J. Hunt, M. Munih, N.d.N. Donaldson, Feedback control of unsupported standing in paraplegia. I. Optimal control approach, IEEE Trans. Rehabil. Eng. 5 (4) (1997) 331–340.
[10] M. Munih, N.d.N. Donaldson, K.J. Hunt, F.M. Barr, Feedback control of unsupported standing in paraplegia. II. Experimental results, IEEE Trans. Rehabil. Eng. 5 (4) (1997) 341–352.
[11] M.J. Dolan, B.J. Andrews, P. Veltink, Switching curve controller for fes-assisted standing up and sitting down, IEEE Trans. Rehabil. Eng. 6 (2) (1998) 167–171.
[12] K.J. Hunt, M. Munih, N. Donaldson, F.M. Barr, Optimal control of ankle joint moment: toward unsupported standing in paraplegia, IEEE Trans. Autom. Control 43 (6) (1998) 819–832.
[13] P.H. Veltink, N. Donaldson, A perspective on the control of fes-supported standing, IEEE Trans. Rehabil. Eng. 6 (2) (1998) 109–112.
[14] R. Kobetic, R.J. Triolo, J.P. Uhlir, C. Bieri, M. Wibowo, G. Polando, E.B. Marsolais, J. Davis, K.A. Ferguson, M. Sharma, Implanted functional electrical stimulation system for mobility in paraplegia: a follow-up case report, IEEE Trans. Rehabil. Eng. 7 (4) (1999) 390–398.
[15] T. Edrich, R. Riener, J. Quintern, Analysis of passive elastic joint moment in paraplegics, IEEE Trans. Biomed. Eng. 47 (8) (2000) 1058–1065.
[16] K.J. Hunt, B. Stone, N.-O. Negard, T. Schauer, M.H. Fraser, A.J. Cathcart, C. Ferrario, S.A. Ward, S. Grant, Control strategies for integration of electric motor assist and functional electrical stimulation in paraplegic cycling: utility for exercise testing and mobile cycling, IEEE Trans. Neural Syst. Rehabil. Eng. 12 (1) (2004) 89–101.
[17] S. Jezernik, R.G. Wassink, T. Keller, Sliding mode closed-loop control of fes controlling the shank movement, IEEE Trans. Biomed. Eng. 51 (2) (2004) 263–272.
[18] M. Mihelj, M. Munih, Unsupported standing with minimized ankle muscle fatigue, IEEE Trans. Biomed. Eng. 51 (8) (2004) 1330–1340.
[19] J.P. Uhlir, R.J. Triolo, J.A. Davis, C. Bieri, Performance of epimysial stimulating electrodes in the lower extremities of individuals with spinal cord injury, IEEE Trans. Neural Syst. Rehabil. Eng. 12 (2) (2004) 279–287.
[20] R. Kamnik, J.Q. Shi, R. Murray-Smith, T. Bajd, Nonlinear modeling of fes-supported standing-up in paraplegia for selection of feedback sensors, IEEE Trans. Neural Syst. Rehabil. Eng. 13 (1) (2005) 40–52.
[21] J.-y. Kim, M.R. Popovic, J.K. Mills, Dynamic modeling and torque estimation of fes-assisted arm-free standing for paraplegics, IEEE Trans. Neural Syst. Rehabil. Eng. 14 (1) (2006) 46–54.
[22] A. Ajoudani, A. Erfanian, A neuro-sliding-mode control with adaptive modeling of uncertainty for control of movement in paralyzed limbs using functional electrical stimulation, IEEE Trans. Biomed. Eng. 56 (7) (2009) 1771–1780.
[23] F. Previdi, M. Ferrarin, I. Carpinella, S. Savaresi, Modelling and control of a device for rehabilitation of paraplegic patients, in: 2007 American Control Conference, IEEE, 2007, pp. 2030–2035.
[24] D. Erol, N. Sarkar, Coordinated control of assistive robotic devices for activities of daily living tasks, IEEE Trans. Neural Syst. Rehabil. Eng. 16 (3) (2008) 278–285.
[25] K.-H. Seo, J.-J. Lee, The development of two mobile gait rehabilitation systems, IEEE Trans. Neural Syst. Rehabil. Eng. 17 (2) (2009) 156–166.
[26] Y. Hasegawa, J. Jang, Y. Sankai, Cooperative walk control of paraplegia patient and assistive system, in: 2009 IEEE/RSJ International Conference on Intelligent Robots and Systems, IEEE, 2009, pp. 4481–4486.
[27] A. Tsukahara, Y. Hasegawa, Y. Sankai, Standing-up motion support for paraplegic patient with robot suit hal, in: 2009 IEEE International Conference on Rehabilitation Robotics, IEEE, 2009, pp. 211–217.
[28] K. Suzuki, G. Mito, H. Kawamoto, Y. Hasegawa, Y. Sankai, Intention-based walking support for paraplegia patients with robot suit hal, Adv. Robot. 21 (12) (2007) 1441–1469.
[29] Y. Stauffer, Y. Allemand, M. Bouri, J. Fournier, R. Clavel, P. Métrailler, R. Brodard, F. Reynard, The walktrainer-a new generation of walking reeducation device combining orthoses and muscle stimulation, IEEE Trans. Neural Syst. Rehabil. Eng. 17 (1) (2008) 38–45.
[30] R.J. Farris, H.A. Quintero, M. Goldfarb, Preliminary evaluation of a powered lower limb orthosis to aid walking in paraplegic individuals, IEEE Trans. Neural Syst. Rehabil. Eng. 19 (6) (2011) 652–659.
[31] S. Viteckova, P. Kutilek, M. Jirina, Wearable lower limb robotics: a review, Biocybern. Biomed. Eng. 33 (2) (2013) 96–105, https://doi.org/10.1016/j.bbe.2013.03.005.
[32] F. Zhang, Z.-G. Hou, L. Cheng, W. Wang, Y. Chen, J. Hu, L. Peng, H. Wang, ileg – a lower limb rehabilitation robot: a proof of concept, IEEE Trans. Human-Mach. Syst. 46 (5) (2016) 761–768.
[33] K.-m. Lee, C.-H. Lee, S. Hwang, J. Choi, Y.-b. Bang, Power-assisted wheelchair with gravity and friction compensation, IEEE Trans. Ind. Electron. 63 (4) (2016) 2203–2211.
[34] M. Geravand, P.Z. Korondi, C. Werner, K. Hauer, A. Peer, Human sit-to-stand transfer modeling towards intuitive and biologically-inspired robot assistance, Autonom. Robots 41 (3) (2017) 575–592.
[35] R. Hari Krishnan, S. Pugazhenthi, Design and development of a robotic self-transfer device for wheelchair users, J. Enabling Technol. 11 (2) (2017) 59–72.
[36] V. Nekoukar, A. Erfanian, A decentralized modular control framework for robust control of fes-activated walker-assisted paraplegic walking using terminal sliding mode and fuzzy logic control, IEEE Trans. Biomed. Eng. 59 (10) (2012) 2818–2827.
[37] S. Page, L. Saint-Bauzel, P. Rumeau, V. Pasqui, Smart walkers: an application-oriented review, Robotica 35 (6) (2017) 1243–1262.
[38] N.A. Ghani, M. Tokhi, Sit-to-stand and stand-to-sit control mechanisms of two-wheeled wheelchair, J. Biomech. Eng. 138 (4) (2016) 041007.
[39] N. Naseer, K.-S. Hong, fnirs-based brain-computer interfaces: a review, Front. Human Neurosci. 9 (2015) 3.
[40] Y.H. Yin, Y.J. Fan, L.D. Xu, Emg and epp-integrated human-machine interface between the paralyzed and rehabilitation exoskeleton, IEEE Trans. Inform. Technol. Biomed. 16 (4) (2012) 542–549.
[41] A. Ferreira, W.C. Celeste, F.A. Cheein, T.F. Bastos-Filho, M. Sarcinelli-Filho, R. Carelli, Human-machine interfaces based on emg and eeg applied to robotic systems, J. NeuroEng. Rehabil. 5 (1) (2008) 10.
[42] M.J. Khan, K.-S. Hong, N. Naseer, M. Bhutta, S. Yoon, Hybrid eeg-nirs bci for rehabilitation using different brain signals, Proc. of the Annual Conference of the Society of Instrument and Control Engineers (SICE) (2014) 1768–1773.
[43] A. Jebri, T. Madani, K. Djouani, Neural adaptive integral-sliding-mode controller with a ssvep-based bci for exoskeletons, 2019 19th International Conference on Advanced Robotics (ICAR) (2019) 87–92.
[44] F. Moldoveanu, Sliding mode controller design for robot manipulators, Bull. Transilvania Univ. Brasov. Eng. Sci. Ser. I 7 (2) (2014) 97.
[45] R. Caton, The Electric Currents of the Brain, 1970.
[46] T. Le, G. Mackellar, Wearable system for detecting and measuring biosignals, US Patent A 10/028,703 (2018).
[47] M.S.b. Abd Rani, W.bt. Mansor, Detection of eye blinks from eeg signals for home lighting system activation, 2009 6th International Symposium on Mechatronics and its Applications (2009) 1–4.
[48] A. Delorme, S. Makeig, Eeglab: an open source toolbox for analysis of single-trial eeg dynamics including independent component analysis, J. Neurosci. Methods 134 (1) (2004) 9–21.
[49] M. Kołodziej, A. Majkowski, R.J. Rak, Linear discriminant analysis as eeg features reduction technique for brain-computer interfaces, Przeglad Elektrotechniczny 88 (2012) 28–30.
[50] A.M. Khan, D.-W. Yun, C. Han, Chattering free sliding mode control of upper-limb rehabilitation robot with handling subject and model uncertainties, J. Inst. Control Robot. Syst. 21 (5) (2015) 421–426.
[51] Y. Luo, C. Wang, Z. Wang, Y. Ma, C. Wang, X. Wu, Design and control for a compliant knee exoskeleton, in: 2017 IEEE International Conference on Information and Automation (ICIA), IEEE, 2017, pp. 282–287.